

COMPUTER SIMULATION OF CATCHING OF EXPLOSIVELY PROPELLING METAL FRAGMENTS BY PROTECTIVE CASING

KAROL JACH
ROBERT ŚWIERCZYŃSKI

Institute of Optoelectronics, Military University of Technology, Warsaw
e-mail: kjach@wat.edu.pl

ADAM WIŚNIEWSKI

Military Institute of Armament Technology, Zielonka
e-mail: zak_18@witu.mil.pl

In the paper a mathematical-physical model, results of computer simulation of the propelling of metal fragments by pressure of detonation products and their catching by the protective casing made of a quasi-aramide fabric have been presented. The impact on the protective casing due to shock waves generated by the explosion has been examined. Depending on the nature of the issue, the 2D free particles or 1D Lagrange method has been used in the computer simulation.

Key words: computer simulation, metal fragments, protective casing

1. Explosive propelling of metal fragments

In order to allow safe detonation of a terrorist bomb, located in a public place, different kinds of the protective casing made of steel, gum, etc. are used.

One of the important problems that must be considered before the construction of such a protective layer is gaining theoretical knowledge about behaviour of the debris during the explosion of the bomb. In this paper, simulation of the explosion has been described as the impact of a fragment propelled by explosion products of a 200 g trinitrotoluene block on the protective casing. The influence of the air shock wave caused by the explosion on the casing and the time of flight of the fragment and of this wave to the

internal surface of the protective layer has been modelled as well. Its is especially important to evaluate the power of the destruction of the casing by the air shock wave during the flight of the fragment to the internal surface of the protective layer. It has been assumed that the protective casing was made of a quasi-aramide fabric.

Because of the lack of literature data concerning the behaviour of the quasi-aramid fabric under dynamic loading, computer simulation has been performed in the way to obtain, on the base of the knowledge of static parameters of this fabric and multiple computer simulations, sufficient matching of experimental results with the results of this simulation. Such a method of computer analysis permits one to choose constants of the equation of state and constitutive relations of the quasi-aramid fabric, and then to proceed with computer simulations with varying input data of the casing in order to optimise its mass, etc.

To describe the behaviour of metals under high dynamic loading during explosive propelling of fragments, a model of elastoplastic body has been used. The system of equations expressing the conservation laws and constitutive relations for this model have the following form (axial symmetry), see Wilkins (1984), Jach *et al.* (2001), Jach and Włodarczyk (1992)

$$\begin{aligned}
 \frac{d\rho}{dt} + \rho \nabla \cdot \mathbf{w} &= 0 \\
 \rho \frac{du}{dt} &= -\frac{\partial p}{\partial r} + \frac{\partial S_{rr}}{\partial r} + \frac{\partial S_{rz}}{\partial z} + \frac{S_{rz} - S_{\varphi\varphi}}{r} \\
 \rho \frac{dv}{dt} &= -\frac{\partial p}{\partial z} + \frac{\partial S_{rz}}{\partial r} + \frac{\partial S_{zz}}{\partial z} + \frac{S_{rz}}{r} \\
 \rho \frac{de}{dt} &= -p \nabla \cdot \mathbf{w} + S_{rr} \frac{\partial u}{\partial r} + S_{\varphi\varphi} \frac{u}{r} + S_{zz} \frac{\partial v}{\partial z} + S_{rz} \left(\frac{\partial u}{\partial z} + \frac{\partial v}{\partial r} \right) \\
 \frac{dS_{rr}}{dt} &= 2\mu \left(\frac{\partial u}{\partial r} - \frac{1}{3} \nabla \cdot \mathbf{w} \right) + \left(\frac{\partial u}{\partial z} - \frac{\partial v}{\partial r} \right) S_{rz} \\
 \frac{dS_{\varphi\varphi}}{dt} &= 2\mu \left(\frac{u}{r} - \frac{1}{3} \nabla \cdot \mathbf{w} \right) \\
 \frac{dS_{zz}}{dt} &= 2\mu \left(\frac{\partial v}{\partial z} - \frac{1}{3} \nabla \cdot \mathbf{w} \right) - \left(\frac{\partial u}{\partial z} - \frac{\partial v}{\partial r} \right) S_{rz} \\
 \frac{dS_{rz}}{dt} &= \mu \left(\frac{\partial u}{\partial z} + \frac{\partial v}{\partial r} \right) - \frac{1}{2} \left(\frac{\partial u}{\partial z} - \frac{\partial v}{\partial r} \right) (S_{rr} - S_{zz})
 \end{aligned} \tag{1.1}$$

The von Mises limit of elasticity is assumed in the form

$$S_{ij} S_{ij} \leq \frac{2}{3} Y^2 \tag{1.2}$$

where

$$S_{ij}S_{ij} = S_{rr}^2 + S_{zz}^2 + S_{\varphi\varphi}^2 + 2S_{rz}^2 \quad (1.3)$$

The equation of state for metals is accepted in the form

$$p = k_1x + k_2x^2 + k_3x^3 + \gamma_0\rho_0e \quad (1.4)$$

$$x = 1 - \frac{\rho_0}{\rho_S} \quad k_2 = 0 \quad \text{if} \quad x < 0$$

The temperature of the metal can be calculated from the relation

$$T = 300 \frac{e_0 - e}{e_{00}} \quad e_0 = e_{00} + e_{01}x + e_{02}x^2 + e_{03}x^3 + e_{04}x^4 \quad (1.5)$$

where: r, z are space coordinates (axial symmetry), t – time, ρ – density, u, v – mass velocity components along the r, z coordinates, p – pressure, e – internal energy, T – temperature, ρ_s – density of the solid phase, S_{ik} – components of the stress deviator, Y – yield strength, μ – shear modulus.

The equation of state in the form of (1.4)₁ is very convenient from the practical point of view because on one hand it is valid in a wide range of the pressure and temperature and on the other hand one can find in literature, see Barbee *et al.* (1972), exact values of the constant coefficients: $k_1, k_2, k_3, e_{00}, e_{01}, e_{02}, e_{03}, e_{04}$ for several most frequently used metals in the related research.

For the description of strength properties of the metals, a modified model using elements of the Steinberg-Guinan and Johnson-Cook models (Johnson and Cook, 1983; Johnson and Lindholm, 1983; Steinberg, 1991; Steinberg *et al.*, 1980; Steinberg and Lund, 1989) is used

$$Y = [A + B(\varepsilon^p)^n](1 + C \ln \varepsilon_*^p)(1 + bp - T_*^m)F(\rho_S)$$

$$[A + B(\varepsilon^p)^n] \leq Y_{max} \quad Y = 0 \quad \text{if} \quad T > T_{m0}$$

$$\mu = \mu_0(1 + bp - T_*^m)F(\rho_S) \quad (1.6)$$

$$\varepsilon^p = \frac{\sqrt{2}}{3} \sqrt{(\varepsilon_{rr}^p - \varepsilon_{zz}^p)^2 + (\varepsilon_{rr}^p - \varepsilon_{\varphi\varphi}^p)^2 + (\varepsilon_{zz}^p - \varepsilon_{\varphi\varphi}^p)^2 + \frac{3}{2}(\varepsilon_{rz}^p)^2}$$

$$F(\rho_S) = \begin{cases} 1 & \text{if } \rho_S \geq \rho_{S1} \\ \frac{\rho_S - \rho_{S2}}{\rho_{S1} - \rho_{S2}} & \text{if } \rho_{S2} \leq \rho_S < \rho_{S1} \\ 0 & \text{if } \rho_S < \rho_{S2} \end{cases}$$

where ε_{ik}^p denotes the components of tensor of plastic strain, ε^p is the intensity of plastic strain, $\dot{\varepsilon}_*^p = \dot{\varepsilon}^p / \dot{\varepsilon}_0^p$ - plastic strain rate for $\dot{\varepsilon}_0^p = 1.0 \text{ s}^{-1}$, $T_* = (T - T_0) / (T_{m0} - T_0)$, T_0 and T_{m0} - initial temperature and the melting point temperature, A, B, C, n, m - material constants.

The system of equations describing the dynamics of the volume increase of microcracks (microvoids) is assumed as in modified Fortow's model (Agiurejkin *et al.*, 1984; Barbee *et al.*, 1972; Johnson, 1981; Sugak *et al.*, 1983)

$$\frac{dV_c}{dt} = \begin{cases} -k \operatorname{sgn} p \left[|p| - \sigma_0 \frac{V_{c1}}{V_c + V_{c1}} \right] (V_c + V_{c0}) & \text{if } |p| \geq \sigma_0 \frac{V_{c1}}{V_c + V_{c1}} \\ 0 & \text{if } |p| < \sigma_0 \frac{V_{c1}}{V_c + V_{c1}} \end{cases} \quad (1.7)$$

$$\frac{1}{\rho} = V_c + \frac{1}{\rho_s} \quad \sigma_0 = \sigma_{00} F(\rho_s) H(\varepsilon^p) (1 - T_*^m)$$

The limitation of the strength properties brought about by appearing microcracks is modeled by multiplying Y , μ and η by the suitable function $G(V_c)$

$$Y^\top = YG(V_c) \quad \mu^\top = \mu G(V_c) \quad (1.8)$$

$$(k_1, k_2, k_3)^\top = (k_1, k_2, k_3)G(V_c)$$

The functions $G(V_c)$ and $H(\varepsilon^p)$ are assumed in the form

$$G(V_c) = 1 - \rho V_c \quad H(\varepsilon^p) = \exp\left(-\frac{1}{2}\varepsilon^p\right) \quad (1.9)$$

2. Equations describing explosive detonation

In the description of processes of an explosive detonation, classical equations of hydrodynamics have been used

$$\begin{aligned} \frac{d\rho}{dt} + \rho \nabla \cdot \mathbf{w} &= 0 & \rho \frac{du}{dt} &= -\frac{\partial p}{\partial r} \\ \rho \frac{dv}{dt} &= -\frac{\partial p}{\partial z} & \rho \frac{de}{dt} &= -p \nabla \cdot \mathbf{w} \end{aligned} \quad (2.1)$$

System of equations (2.1) was then completed by the equation of state of detonation products. It was assumed in the form of JWL

$$p_{PD} = A \left(1 - \frac{\delta}{R_1 V}\right)^{-R_1 V} + B \left(1 - \frac{\delta}{R_2 V}\right)^{-R_2 V} + \delta \rho e \quad (2.2)$$

where $V = \rho_0/\rho$; A, B, R_1, R_2, δ denote empirical constants.

The system of equations mentioned above was applied in all cases, in which so-called "detonative optics" approximation was used, i.e. when the knowledge of the detonation wave front shape and of parameters on its front (Chapman-Jouguet's parameters) was assumed.

3. Behaviour of protective casing under pressure of detonation products and shock wave in the air

To describe the process of protective casing deformation one can use a system of equations for an elastic solid in the spherical symmetry, see Stanyukovic (1975)

$$\begin{aligned}
 \frac{dp}{dt} + \rho \nabla \cdot \mathbf{w} &= 0 \\
 \rho \frac{du}{dt} &= -\frac{\partial p}{\partial r} + \frac{\partial S_1}{\partial r} + 2\frac{S_1 - S_2}{r} \\
 \rho \frac{de}{dt} &= -p \nabla \cdot \mathbf{w} + S_1 \frac{\partial u}{\partial r} + 2S_2 \frac{u}{r} \\
 \frac{dS_1}{dt} &= 2\mu \left(\frac{\partial u}{\partial r} - \frac{1}{3} \nabla \cdot \mathbf{w} \right) \\
 \frac{dS_2}{dt} &= 2\mu \left(\frac{u}{r} - \frac{1}{3} \nabla \cdot \mathbf{w} \right)
 \end{aligned} \tag{3.1}$$

where

$$\nabla \cdot \mathbf{w} = \frac{\partial u}{\partial r} + 2\frac{u}{r} \tag{3.2}$$

The system of equations of the problem was then completed by the equation of state in the form of

$$p = K \left(1 - \frac{\rho_0}{\rho} \right) \tag{3.3}$$

The stresses were calculated as follows

$$\sigma_1 = -p + S_1 \quad \sigma_2 = -p + S_2 \tag{3.4}$$

where: σ_1 stands for the radial stress, σ_2 - longitudinal stress, K - bulk modulus, μ - shear modulus.

4. Model of deceleration of steel fragments in the air

The equation describing motion of metal fragments in the air has been assumed in the following form

$$m \frac{dv}{dt} = -\frac{1}{2} c \rho_a v^2 s \quad m = \frac{4}{3} \pi \left(\frac{D}{2} \right)^3 \rho_s \quad (4.1)$$

where: D is the diameter of the steel ball, s – surface of the body ($s = \pi D^2/4$), v – velocity of the ball, ρ_a – density of the air, ρ_s – density of steel, m – mass of the steel ball.

The coefficient c was approximated as follows (Cerný, 1988)

$$c = -0.2 \left(\frac{\text{Re}}{10^5} \right) + 0.7 \quad (4.2)$$

where Re is the Reynold's number

$$\text{Re} = \frac{\rho_p v D}{\eta}$$

5. Constant coefficients of materials used in calculations

The coefficients determining material properties of the examined bodies are presented in the Table 1 and Table 2.

Table 1. Coefficients of the equation of state JWL for trinitrotoluene

| | | | | | |
|-------------------------------|------|-----------|-------|--------------------|------|
| ρ_0 [g/cm ³] | 1.63 | A [GPa] | 373.8 | R_2 | 0.9 |
| D [m/s] | 6930 | B [GPa] | 3.747 | δ | 0.35 |
| p_{CJ} [GPa] | 21.0 | R_1 | 4.15 | $\rho_0 e_0$ [GPa] | 5.9 |

For the casing one has $K = 8.8$ GPa, $\mu = 300$ GPa, $Y = 0.1$ GPa, $p_{min} = -0.3$ GPa, $\rho_{cr} = 0.5\rho_0$ (p_{min} and ρ_{cr} represent the critical pressure and density values at tearing the quasi-aramide fabric). The air viscosity $\eta = 3 \cdot 10^{-4}$ g/(cm·s) has been assumed in the calculation.

To simulate the penetration of the quasi-aramide casing by a propelled metal fragment, equations (1.1)-(1.3) of elastoplastic body were used. In this case, for the quasi-aramide fabric, a simplified strength model was applied: $Y = \text{const}_1$ and $\mu = \text{const}_2$, in the plasticity area.

Table 2. Values of coefficients occurring in the equation of state, in the model of microcracks formation and in the Johnson-Cook model for steel

| | | | |
|-------------------------------|---------------------|----------------------------------|----------------------|
| ρ_0 [g/cm ³] | 7.9 | C | 0 |
| γ_0 | 2.17 | m | 0.55 |
| k_1 [GPa] | 164.8 | n | 0.32 |
| k_2 [GPa] | 312.4 | Y_{max} [GPa] | 2.0 |
| k_3 [GPa] | 564.9 | T_{m0} [K] | 1811 |
| ε_{00} [J/g] | $-1.340 \cdot 10^2$ | k [1/(Pa·s)] | 0.25 |
| ε_{01} [J/g] | $-2.908 \cdot 10^2$ | σ_0 [GPa] | 2.5 |
| ε_{02} [J/g] | $1.012 \cdot 10^4$ | μ_0 [GPa] | 77 |
| ε_{03} [J/g] | $2.051 \cdot 10^4$ | V_{C0} [cm ³ /g] | $1.27 \cdot 10^{-5}$ |
| ε_{04} [J/g] | $2.901 \cdot 10^4$ | V_{C1} [cm ³ /g] | $6.33 \cdot 10^{-4}$ |
| A [GPa] | 344 | ρ_{S1} [g/cm ³] | 6.87 |
| B [GPa] | 680 | ρ_{S2} [g/cm ³] | 5.84 |

6. Analysis of calculations results

Figure 1 presents a sequence of snapshots of the process of propelling of the standard steel fragment of about 1.1 g, located on a 90 mm long, 200 g trinitrotoluene block.

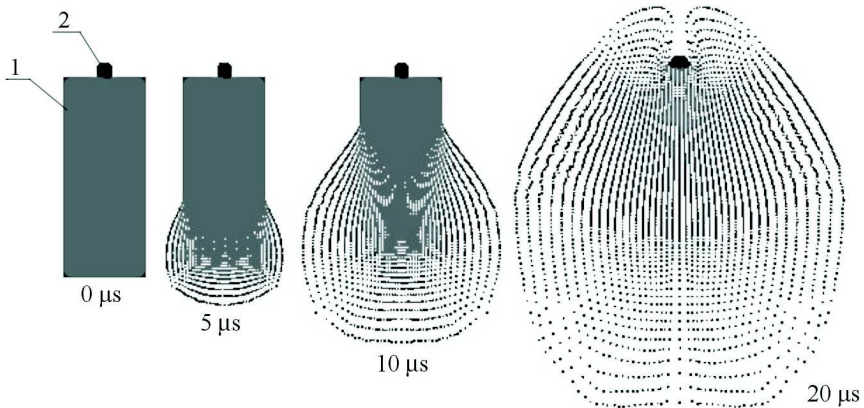


Fig. 1. Snapshot sequence of the standard steel fragment propelling process. The results were obtained using the free particle method (Jach *et al.*, 2001). Initial distance of trinitrotoluene block (1) from metal fragment (2) is 90 mm

The fragment, propelled explosively, reaches the velocity of about 800 m/s (Fig. 2). A change in the velocity caused by deceleration in the air, and the increasing range of the fragment in time for different initial velocities are shown in Fig. 3. For ranges of the order of 0.5-1.0 m, the deceleration due to the air is negligible.

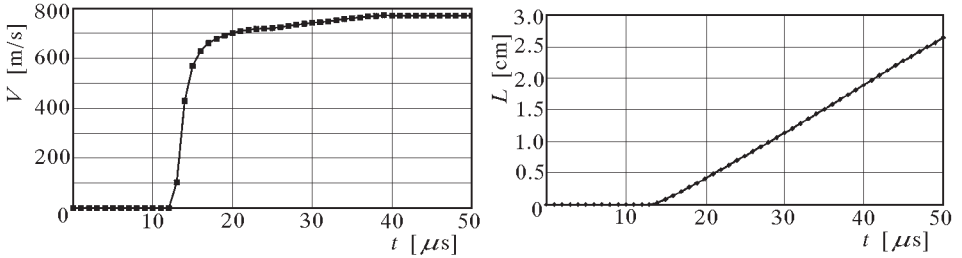


Fig. 2. Velocity V and range L of the fragment propelled by products of detonation (the initiation as in Fig. 1) as a function of time t (since the initiation of detonation)

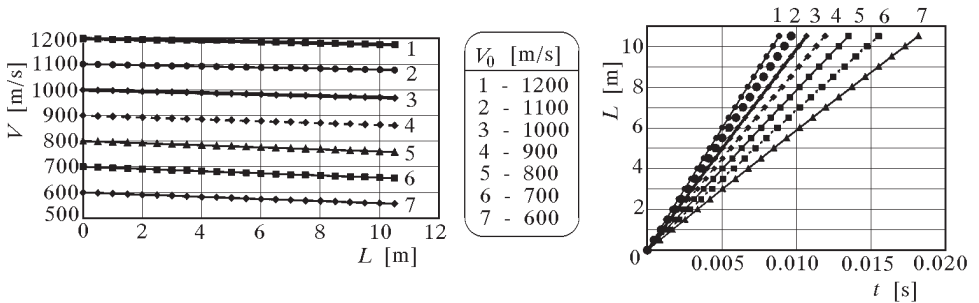


Fig. 3. Changes of velocity V and range L of fragments during motion in the air for different initial velocities V_0

As a result of detonation of the trinitrotoluene block, the shape of the propelled fragment becomes a little deformed plastically in the first phase of the propelling, when the pressure of detonation products exceeds the yield strength (Fig. 4).

Figure 5 shows additionally changes of the energy density of the fragment for different initial velocities (as a result of deceleration in the air). In the distance of several metres from the explosion, the energy density still significantly exceeds the value which is assumed as dangerous for human life, i.e. 100-150 J/cm².

The following figures present basic characteristics concerning the process of shock wave propagation in the air and of its influence on the protective

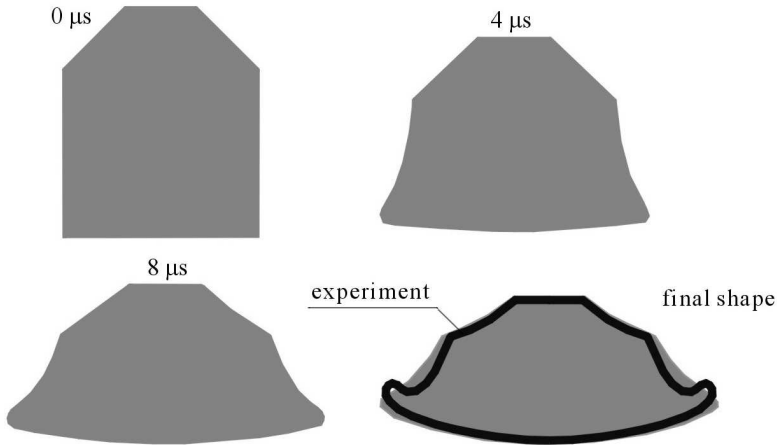


Fig. 4. The shape of the propelled fragment. Results of the computer simulations based on the free particles method

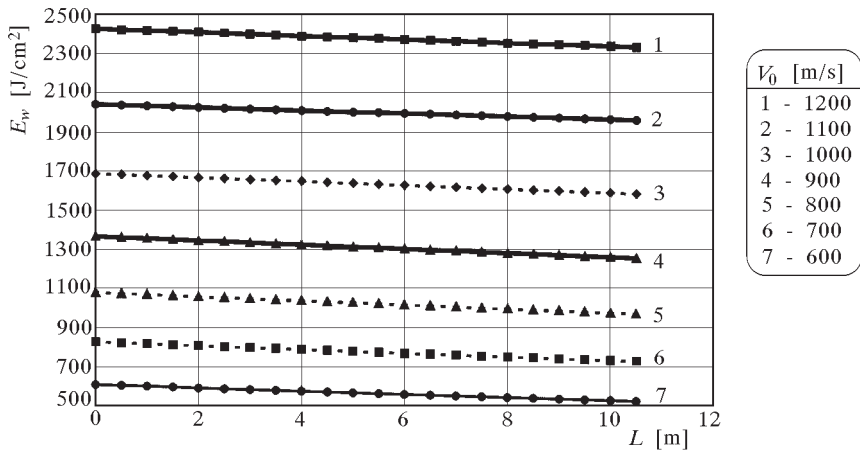


Fig. 5. Energy density E_w of fragments as a function of their range L in the air

casing. The results have been obtained using the Lagrange method. Changes of the pressure on the shock wave front in the air are shown in Fig. 6. This wave reaches the surface of the internal protective casing and, as a result of reflection from it, significantly increases its own amplitude. The change of the pressure on the edge of the protective casing in function of time is presented in Fig. 7. The second, moderate local maximum of the pressure results from reaching the edge by the secondary shock wave reflected from the border: products of detonation – the air.

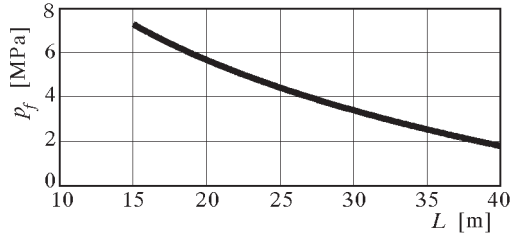


Fig. 6. The pressure at the shock wave front in the air as a function of its range

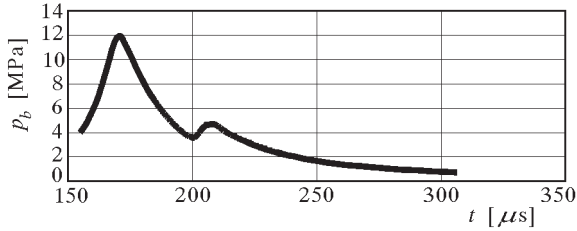


Fig. 7. The pressure on the internal surface of the protective casing as a function of time

The maximum tensile stresses, stretching the casing as a result of the pressure action (Fig. 7), occur on the internal edge of the protective layer. The changes of the tensile stresses in time are presented in Fig. 8.

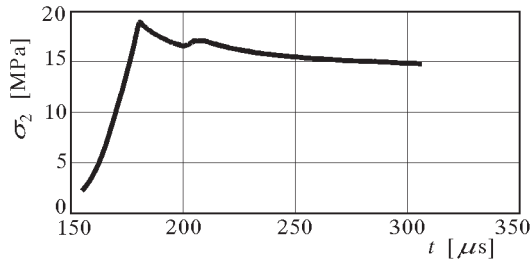


Fig. 8. Longitudinal tensile stress on the internal surface of the protective casing

Another important issue is also the problem of the time required by the air shock wave and fragments to reach the protective casing. Changes of the range of the shock wave and of the propagating fragment (with the velocity of 800 m/s) are illustrated in Fig. 9. From this figure it results that the shock wave in the air overtakes the fragment significantly. In the time of about

$160 \mu\text{s}$ the shock wave reaches the edge of the protective layer (with the radius of 400 mm), and in this time the fragment travels a distance of only about 120 mm.

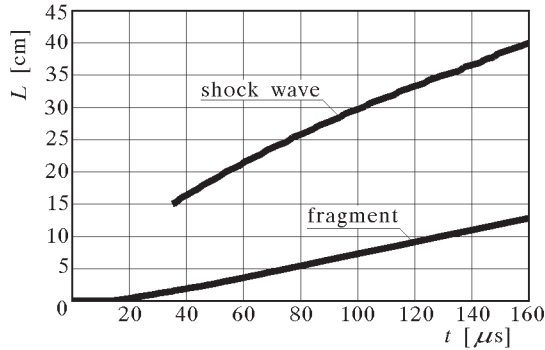


Fig. 9. Comparison of the range of the shock wave in the air with the range of the steel fragment

The multilayered fabric is impacted by a random side of the propelled fragment. In order to evaluate the catching properties of the casing, the standard cylindrical fragment was used in the calculations. Figure 10 shows results of computer simulation, based on the free particles method, of penetration of the protective fabric by a steel fragment propelled to the velocity of 900 m/s (the last picture refers to the moment when the fragment has been completely stopped). As one can see, during the penetration of the protective casing, the fragment is hardly deformed.

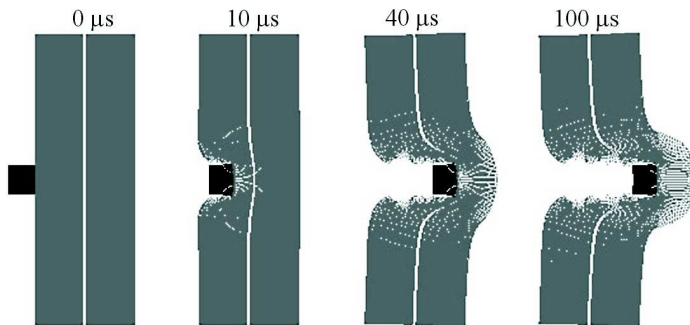


Fig. 10. Computer simulation of penetration of the protective multilayered fabric by the steel fragment

Figure 11 shows the decrease of the steel fragment velocity as a result of its interaction with the protective fabric for three different values of velocities of the impact of the fragment.

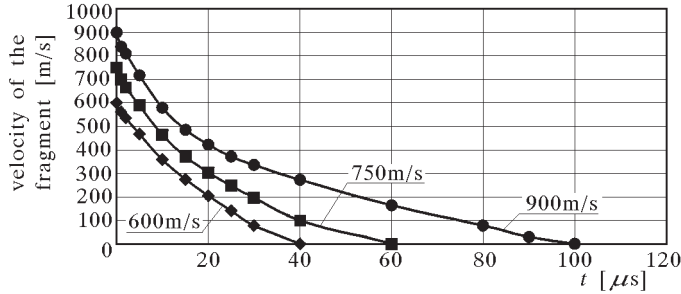


Fig. 11. The decrease of the velocity of the steel fragment as a result of deceleration in the protective fabric for three different values of velocities of the impact of the fragment – results of calculations obtained using the free particles method

7. Conclusions

The following remarks can be formulated based on the results of computer simulations carried out throughout the work:

- The time that the shock wave needs to reach the inner surface of the protective casing is significantly shorter than the analogous time pertaining to the fragment.
- The change of the fragment shape, i.e. mushrooming of the surface of the fragment is caused by the pressure impact of the explosion products. It does not occur during the penetration through the protective casing.
- It is possible to select appropriate input data in the calculations so that the simulation results would agree with the results of the experiment (e.g. the depth of the protective casing penetration occurred to be in line with the experimental results).
- The computer codes used can be applied to optimisation of parameters of the protective casing, i.e. its thickness, sensitivity to the kind, shape and mass of the explosive as well as the kind, shape and mass of the propagating fragments.

References

1. AGUREĪKIN V.A., ANISIMOV S.I., BUSHMAN A.V., KANEL G.I., KARYAGIN V.P., KONSTANTINOV A.B., KRYUKOV B.P., MININ V.F., RAZORENOV S.V., SAGDEEV R.Z., SUGAK S.G., FORTOV V.E., 1984, Thermophysical and gas dynamics problems of protection against meteors of the Vega space vehicle [in Russian], *Teplofizika Vysokikh Temperatur*, **22**, 5
2. BARBEE T.W. JR., SEAMAN L., CREWDSON R., CURRAN D.R., 1972, Dynamic fracture criteria for ductile and brittle metals, *J. Mater. Sci.*, **7**, 393-401
3. CIERNYĀ G.G., 1988, *Gas dynamics* [in Russian], Science, Moscow
4. JACH K., MORKA A., MROCZKOWSKI M., PANOWICZ R., SARZYŃSKI A., STĘPNIEWSKI W., ŚWIERCZYŃSKI R., TYL J., 2001, *Computer modelling of dynamic interaction of bodies by free particles method* [in Polish], PWN
5. JACH K., WŁODARCZYK E., 1992, Solutions of the initial-value problems of the viscoplastic – nonstationary theory for the description shaped charge jet formation and target penetration, *Proceedings of 13th International Symposium on Ballistics, Ballistics'92*, Stockholm, Sweden
6. JOHNSON J.N., 1981, Dynamic fracture and spallation in ductile solids, *J. Appl. Phys.*, **52**, 4, 2812-2825
7. JOHNSON G.R., COOK W.M., 1983, A constitutive model and data for metals subjected to large strains and high temperatures, in: *7th Int. Symposium on Ballistics*, Hague
8. JOHNSON G.R., LINDHOLM U.S., 1983, Strain-rate effects in metals at large shear strains, Material behavior under high stress and ultrahigh loading rates, *Proc. 29th Sagamore Army Mater. Res. Conf.*, Lake Placid 1982, New York
9. STANYUKOVIC K., 1975, *Physics of explosion* [in Russian], Science, Moscow
10. STEINBERG D.J., 1991, Equation of state and strength properties of selected materials, Lawrence Livermore Nat. Lab. UCRL-MA-106439
11. STEINBERG D.J., COCHRAN S.G., GUINAN M.W., 1980, A constitutive model for metals applicable at high-strain rate, *J. Appl. Phys.*, **51**, 3, 1498-1504
12. STEINBERG D.J., LUND C.M., 1989, A constitutive model for strain rates from 10^4 to 10^6 s^{-1} , *J. Appl. Phys.*, **65**, 4, 1528-1533
13. SUGAK S.G., KANEL G.I., FORTOV V.E., NI A.L., STELMAH B.G., 1983, Numerical modelling of the action of an explosion on an iron plate [in Russian], *FGV*, **19**, 2
14. WILKINS M.L., 1984, Modelling the behaviour of materials. Structural impact and crashworthiness, *Proc. Intern. Conf.*, **2**, London, New York

Komputerowa symulacja wychwytywania przez warstwę ochronną metalowych odłamków napędzonych wybuchem

Streszczenie

W pracy przedstawiono matematyczno-fizyczny model oraz wyniki symulacji komputerowych napędzania metalowych odłamków przez produkty detonacji i wychwytywania ich przez warstwę ochronną wykonaną z tkaniny paradramidowej. Przeanalizowano również wpływ generowanej wybuchem fali uderzeniowej w powietrzu na przebieg zachodzących procesów. W zależności od charakteru tych cząstkowych zagadnień wykorzystywano do symulacji komputerowej kody typu 2D (metoda punktów swobodnych) lub 1D (metoda Lagrange'a).

Manuscript received July 10, 2003; accepted for print September 25, 2003